A Continuous Particle/Cell Sorter Using Dielectrophoresis

G. R. Wang, J.J. Feng; S. B. Vasantgadkar, K. Pant; B. Prabhakarpandian, S. Krishnamoorthy, S. Sundaram
CFD Research Corporation
215 Wynn Drive, Huntsville, AL 35806
Email: sxs@cfdrc.com

ABSTRACT

We present the design and experimental results of a novel, continuous, microfluidic sorter for separation of cells or particles by the use of conventional dielectrophoresis (DEP). A high-fidelity modeling and simulation approach was used to guide device design and performance optimization. A laboratory prototype was developed using plastic laminates-based microfabrication. The sorter was experimentally demonstrated for size-based separation of 1 and 5.7μm particles as well as property-based separation of the 5.7μm polystyrene beads and *Bacillus subtilis* vegetative cells. Experimental results matched qualitatively and quantitatively with model predictions.

Keywords: dielectrophoresis, simulation-based modeling, size-based separation, property-based separation

1 INTRODUCTION

Controlled manipulation of biological and non-biological particles is of wide interest in biodefense and biodiagnostic applications. For instance, separation of biotic and abiotic particles in contaminated, "dirty" samples is critical to enhancing the performance (by increasing the sensitivity and selectivity) of current biosensors. In clinical applications, cell separation can make possible life-saving procedures, such as removal of metastatic cells (Gross et al., 1995).

Dielectrophoresis (DEP) has emerged as a promising method for a variety of engineering applications involving micro- and nano-particles (Durr et al. 2003). DEP arises from electrostatic force experienced by polarized particles in a non-uniform electric field, It has been demonstrated for manipulation of non-biological (latex, glass, etc.) as well as biological particles such as cells, bacteria and viruses. DEP provides a novel, label-free technique compared with traditional methods.

While the literature reports several instances of DEP use in selective screening of biologicals (for example Li et al., 2005), the vast majority of the uses are in "batch-mode" devices which trap the targets near electrodes. Complex elution protocols are necessary to flush out the trapped biologicals. In contrast, we report on the development of a novel DEP-based sorter capable of continuous particle separation. The present device is developed in a microfluidics-based format, which would facilitate ease of integration with current and next-generation biodetection platforms.

The DEP force on a particle depends on the arrangement of the electrode and the resulting electric field distribution as well as the dielectric properties of particles and the surrounding medium. This leads to several possible electrode array designs configurations that can be used for particle manipulation and separation based on the electric properties of the particle. Furthermore, since the DEP force is proportional to the volume of the particle, it is also feasible to separate a polydisperse mixture of particles based on particle size. Thus, there are several modalities through which DEP can be employed for the separation of a mixture of particles with different properties and/or size. In this paper, we present the results on the development of a continuous separation device that is capable of sorting particle of different sizes and/or properties. A high-fidelity, multi-physics simulation tool is used to design and characterize the performance under appropriate operation conditions. The optimized device was prototyped using state-of-the-art microfabrication techniques. Device performance was characterized via experimental testing with polystyrene latex (PSL) beads and *Bacillus subtilis* vegetative cells. The sorter was experimentally demonstrated for size-based separation of 1 and 5.7μm particles as well as property-based separation of 5.7μm polystyrene particle and bacterial cells.

2 METHODS

2.1 Modeling of Dielectrophoresis

To predict the DEP response of cells and non-biological particles, we first need to develop suitable models to describe the interactions of particles or cells with non-uniform electric field and fluid flow. Basic models for electric field and fluid flow in DEP-based microsystems have been developed by our group (Feng et al. 2002) and others (see Li et al. 2005) and are discussed only briefly here. To understand particle or cell motion in the presence of non-uniform electric fields, we also need to model the response of particle to electric fields. In this study, we used a homogeneous spherical particle model for non-biological particles (PSL beads) and a layered spherical particle model for cells. Based on these particle models, we can derive the expressions for time-averaged DEP force in an AC electric field as

$$\langle \mathbf{f} \rangle = 2\pi \,\mathrm{Re}\left[\varepsilon_m \varepsilon_0\right] a^3 \,\mathrm{Re}[K(\omega)] \nabla \left|\mathbf{E}_{\mathrm{rms}}\right|^2 \qquad (1)$$

Here σ and ε are physical conductivity and permittivity and the subscript *m* denotes the surrounding media. Later the subscript *in* will be used to denote either cytoplasm or

particle. ε_0 is the permittivity of the vacuum, a is radius of the particle, and K is the Clausius- Mossotti factor. It can be expressed in terms of complex electric properties as

$$K = \left[\frac{Z_2 Z_1 - 1}{Z_2 Z_1 + 2} \right] \quad (2)$$

for non-biological particles and

$$K = \frac{((\lambda^3 + 2)Z_2 - \lambda^3 + 1)Z_1 + (2\lambda^3 - 2)Z_2 - 2\lambda^3 - 1}{((\lambda^3 + 2)Z_2 + 2\lambda^3 - 2)Z_1 + (2\lambda^3 - 2)Z_2 + 4\lambda^3 + 2} \quad (3)$$

for cells. Here

$$Z_1 = \frac{\sigma_{in} + i\omega\varepsilon_0\varepsilon_{in}}{\sigma_m + i\omega\varepsilon_0\varepsilon_m}, Z_2 = \frac{\sigma_m + i\omega\varepsilon_0\varepsilon_m}{\sigma_{out} + i\omega\varepsilon_0\varepsilon_{out}} \quad (4)$$

and λ is the ratio of the outer and inner membrane radii.

Once the DEP force applied to each particle/cell is calculated, its position can be traced from initial configuration by solving

$$m_{p,c} \frac{d\mathbf{u}}{dt} = \langle \mathbf{f} \rangle_{DEP} + \mathbf{f}_h, \mathbf{u} = \frac{d\mathbf{s}}{dt} \quad (5)$$

with initial condition

$$\mathbf{u}(t=0) = \mathbf{u}_0, \mathbf{s}(t=0) = \mathbf{s}_0$$

Here m_w is the mass of each particle/cell; $\mathbf{f}_h$ is the hydrodynamic force on the particle and $\boldsymbol{s}$ is position. We have assumed that:

- Particles are small compared to scale of field non-uniformity
- Particle/cell density is low and the inter-particle/cell effects can be neglected;
- Inertial force, history force (Basset force) are neglected;
- Particle/cell-boundary interaction is neglected

The hydrodynamic force is obtained from Stokes equation as

$$\mathbf{f} = 6\pi\mu\mathbf{u}a \quad (6)$$

The simulations were carried out using CFD-ACE+, a general-purpose Computational Fluid Dynamics (CFD) code (ESI-CFD, Huntsville, AL). CFD-ACE+ employs a finite volume method to numerically solve all the governing equations subjected to appropriate boundary and initial conditions. The operation condition as well as device geometry can be optimized once we define a target function to be maximized. In the present study, we use separation efficiency as our target function.

2.2 Prototype Microfabrication

The electrokinetic chip for DEP sorter was microfabricated by ALine, Inc. (Redondo Beach, CA) using plastic laminates based technology. The top and the bottom layers were constructed from 1 mil (25 μm) acrylic transfer adhesive mounted on 0.5 mil polyethylene terepthalate (PET). The middle layer was constructed from 3 mil transfer adhesive. The top and bottom outlets were constructed from 1.6 mm acrylic to allow interface between the flow cell and the syringe pump used to drive the sample. The electrodes were made out of Indium Tin Oxide (ITO) and patterned on glass slides using a UV laser with resolution to 10 μm. The glass slides were bonded together with laminates to form the component card. Electrical access to the active region was provided by fabricating contact pads near the edge of the chip. Fluidic access to the chip was made available by the use of 1/16″ PEEK tubing.

2.3 Experimental Testing

A schematic of the setup used for DEP sorter experiential testing is shown in Figure 1. Fluorescent polystyrene particles (Polysciences, Inc.) of 1 and 5.7μm diameter were used as abiotic particles. To avoid particle sedimentation, the suspension buffer density was modified by dissolving 12.4% w/w of HPLC grade inositol (Fisher Scientific) in deionized (DI) water. In addition, 1% Bovine Serum Albumin (BSA, Fisher Scientific) was also added to the suspension buffer to eliminate/reduce particle adhesion to the channel walls. The median conductivity of the suspending medium was measured to be 107μS/cm. *Bacillus subtilis* vegetative cells were used as representative biotic particles. The peak-to-peak voltage range for the applied electric voltage was 20V. The applied frequency is in the range of 100kHz–10MHz.

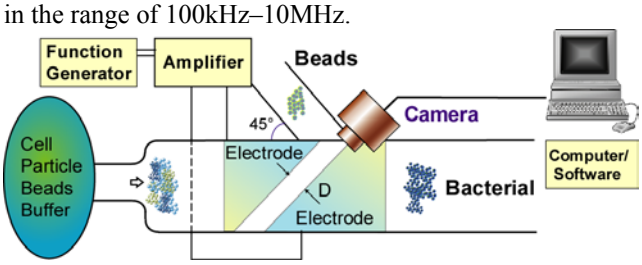

Figure 1. Sketches of separation chamber and the experiment protocol. The electrodes are fabricated on both top and bottom of the channel walls.

3 RESULTS & DISCUSSION

Figure 2a shows a top view of the schematic of the microfluidic device. There are two electrodes in a wedge format on the bottom and top surfaces of the microchannel respectively. The front two electrodes share the same electric signal and the rear two electrodes will share another electric signal. These two AC electric signals have a phase difference of 180°. At one side of the channel, near the electrode gap, a side channel is placed for carrying the migratory particles that experience a larger DEP force. The operational principle is as follows. Upon entering the electrode region, levitative negative DEP forces the particles to the center of the channel in the transverse direction. Subsequently, as these particles approach the gap between the electrode pairs, they experience a strong

negative DEP (Figure 2(b)). The net force of DEP and hydrodynamics pushes the responsive particles to the side channel. The chip is so designed that without electrode activation, 80% of the particles move downstream of the main channel and the other 20% flow through the side channel due to hydrodynamic splitting.

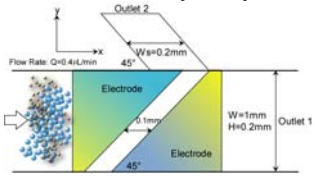

Figure 2(a). Sketch of the prototype design of the DEP sorter

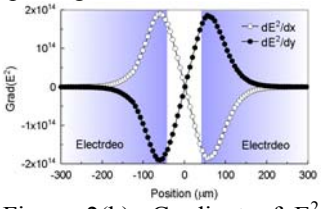

Figure 2(b). Gradient of E^2 across the electrode gap in the middle of the channel

In all the results reported here, the frequency used is 10 MHz. Figure 3 shows the visualization of the deflection of the fluorescent polystyrene particles of 5.7μm diameter for separation to the side channel due to DEP force. The voltage used in Figure 3b was 20Vp-p. The flow rate in Figure 3 was 0.5μL/min. In figure 3a, approximately 80% of the particles flow downstream of the electrodes to the main channel without electrode activation. However, with the activation of the electrodes, almost all particles migrate to the side channel under DEP force as shown in Figure 3b.

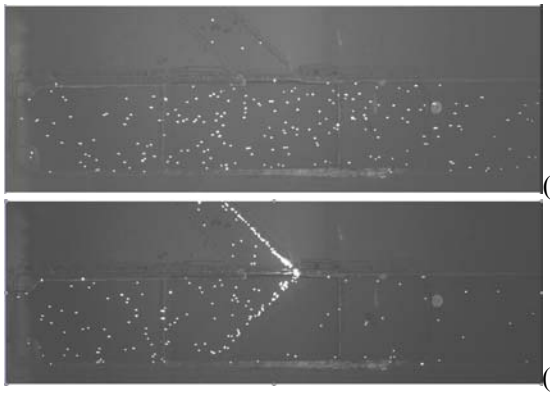

(a)

(b)

Figure 3. Experimental demonstration of the DEP deflection. (a) No AC activation and most particles move downstream of the main channel. (b) With AC activation, almost all particles were repelled to the side channel due to DEP force.

Separation efficiency calculated from these experimental images, as a function of sample flow rate (20Vp-p) is shown in Figure 4. As expected from theoretical and computational analyses, the efficiency decreases with the flow rate, since the hydrodynamic force experienced by the particles increases with an increase in flow rate. When the flow rate was less than 0.4μL/min, the deflection efficiency was 98%, indicating that the DEP forces were larger than the hydrodynamic forces. However, as the flow rate increases to 2μL/min, the hydrodynamic force overwhelms DEP with resultant minimal deflection of the particles. The effect of applied voltage on the separation efficiency is shown in Figure 5. As expected from theory (equation 1), the efficiency increases with an increase in the applied electric field (or equivalently voltage). The flow rate in Figure 5 was maintained at 0.4 μL/min.

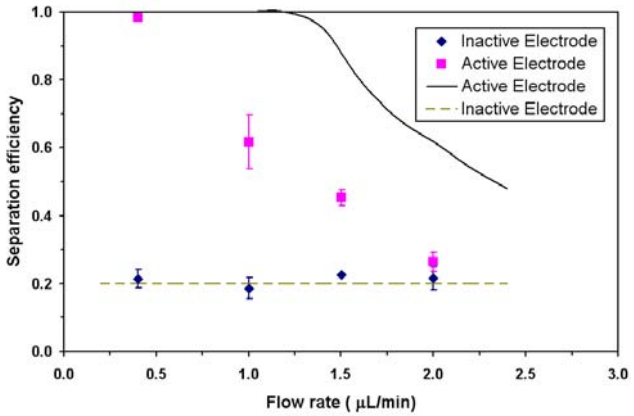

Figure 4. Separation efficiency as a function of sample flow rate. Experimental measurements (symbols) and computational predictions (lines) are shown. Three repeated experimental results were used for the error bar estimation.

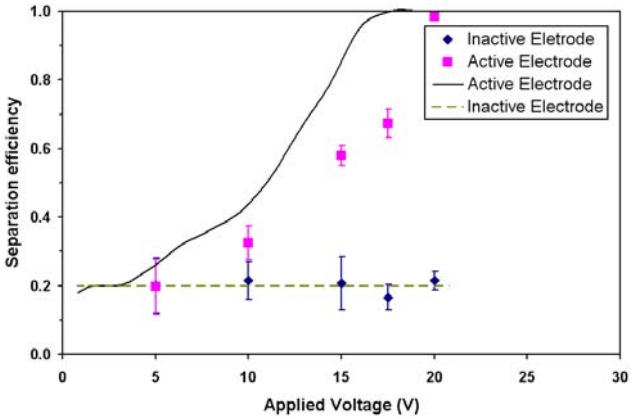

Figure 5. Separation efficiency as a function of applied voltage. Experimental measurements (symbols) and computational predictions (lines) are shown. Three repeated experimental results were used for the error bar estimation.

In Figure 6, we compare the experimentally observed size-based separation of PSL beads with results predicted by the simulational analysis. These experiments were conducted by injecting a mixture of 1 and 5.7μm particles in the DEP sorter. When the electrode is not activated, 80% of both 5.7 and 1μm particles flow along the main channel due to hydrodynamic forces. However, upon activation of electrodes the 5.7μm particles experience DEP forces greater than the hydrodynamic force and are pushed into the side channel, while the 1μm particles continue to flow along the main channel. Figure 6a and 6c show the experimental results without and with electrode activation and Figure 6b and 6d show the corresponding simulation results.

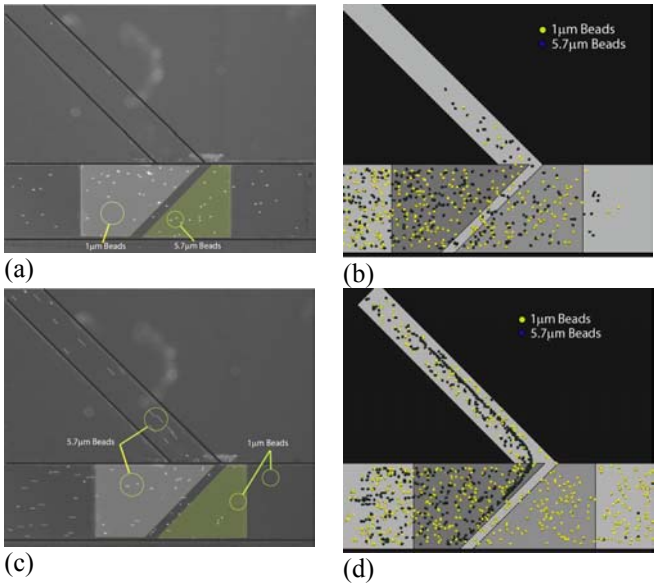

Figure 6. Visualization and comparison of experimental observations (a, c) and simulation predictions (b, d) when particles of 5.7μm and 1μm diameter are injected at flow rate of 0.5 μL/min. (a), (b) Before electrode activation. (c), (d) After electrode activation.

An estimate of the separation efficiency can be obtained from the computational analyses. The separation efficiency of the microparticles of 5.7μm from the 1μm in the main channel is shown in Figure 7. With and without the electrode activation, the separation of 5.7μm particles into the side channel was 96% and 20% respectively. These separation efficiencies were sought to be corroborated with experimental measurements. However, the fluorescence signal measured from the 1μm particles was not sufficient to allow for a precise experimental measurement of size-based separation efficiency.

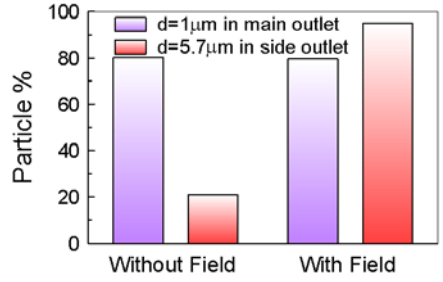

Figure 7. Computational prediction of size-based separation in the DEP sorter.

Finally, the separation of 5.7μm polystyrene particles from the bacterial cells (*Bacillus subtilis*) is demonstrated experimentally in Figure 8. Figure 8a shows the experiment without electrode activation. Both 5.7μm particles and bacterial cells mostly flow unimpeded along the main channel. When the electrodes are activated, almost all of the 5.7 μm particles flowed into the side channel while bacterial cells continue flowing in the main channel as shown in Figure 8b. Since the fluorescence intensity was relatively low for the fluorescently labeled bacteria, amplified pictures are shown in Figure 8c and 8d corresponding Figure 8a and 8b respectively for detailed view near the side channel, for clarity.

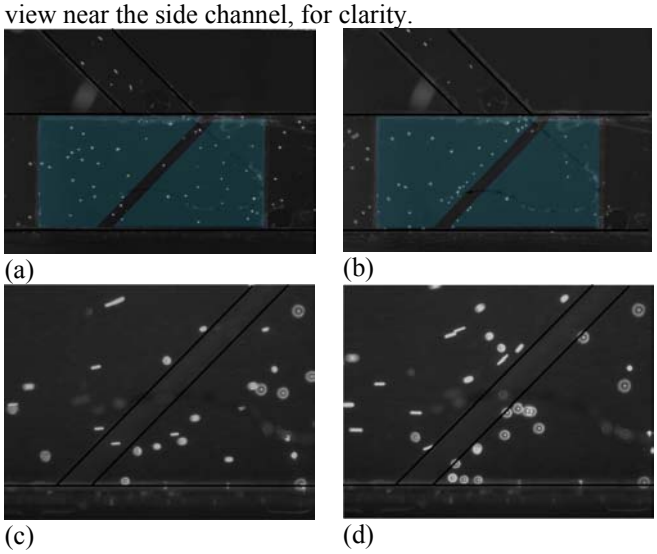

Figure 8. Separation of 5.7 μm Particle and *Bacillus subtilis* cells in the DEP sorter. (a) Before electrode activation, (b) after electrode activation, (c) and (d) details of (a) and (b) near side channel entrance.

4 CONCLUSION

We have designed and experimentally demonstrated a novel microfluidic dielectrophoresis (DEP) based sorter for continuous separation of particles and biological cells. The theoretical concept was extensively investigated using sophisticated, multi-physics models, featuring hydrodynamics, electrokinetics, and particle transport. Prototypes were microfabricated using plastic laminate technology. Separation characteristics of both polystyrene particles and microbial cells (*Bacillus subtilis*) were studied experimentally. Experimental observations on the effect of parameters such as flow rate and applied voltage matched very well with our model predictions. Separation of 5 μm particles in the presence of smaller 1 μm particles or *Bacillus subtilis* cells was demonstrated.

ACKNOWLEDGMENT

The authors gratefully acknowledge research support from the Department of Defense (MARCORSYSCOM, Contract #M67854-04-c-5020) and the Department of Homeland Security (HSARPA, Contract #NBCHC050114). The bacterial cells were graciously provided by Prof. G. Podilla of the University of Alabama, Huntsville.

REFERENCES

1. Dürr, M., et al. *Electrophoresis.* 2003, **24**, 722.
2. Park, J., et al. *Lab on a Chip.* 2005, **5**, 1264.
3. Gross, H., et al. *Proc. Natl. Acad. Sci.* 1995, **92**, 537.
4. Li, H. et al. *J. MEMS* 2005, **14**, 103.
5. Feng, J., et al. *Proc. Mod. Sim. Microsystems,* 2002